

Crystal Nucleation in the Hard-Sphere System Revisited: A Critical Test of Theoretical Approaches

Gyula I. Toth, and Laszlo Granašy

J. Phys. Chem. B, **2009**, 113 (15), 5141-5148 • DOI: 10.1021/jp8097439 • Publication Date (Web): 25 March 2009

Downloaded from <http://pubs.acs.org> on April 23, 2009

More About This Article

Additional resources and features associated with this article are available within the HTML version:

- Supporting Information
- Access to high resolution figures
- Links to articles and content related to this article
- Copyright permission to reproduce figures and/or text from this article

[View the Full Text HTML](#)

Crystal Nucleation in the Hard-Sphere System Revisited: A Critical Test of Theoretical Approaches

Gyula I. Tóth*

Research Institute for Solid State Physics and Optics, H-1525 Budapest, POB 49, Hungary

László Gránásy

Brunel Centre for Advanced Solidification Technology, Brunel University, Uxbridge, Middlesex UB8 3PH, United Kingdom

Received: November 4, 2008; Revised Manuscript Received: January 11, 2009

The hard-sphere system is the best known fluid that crystallizes: the solid–liquid interfacial free energy, the equations of state, and the height of the nucleation barrier are known accurately, offering a unique possibility for a quantitative validation of nucleation theories. A recent significant downward revision of the interfacial free energy from $\sim 0.61kT/\sigma^2$ to $(0.56 \pm 0.02)kT/\sigma^2$ [Davidchack, R.; Morris, J. R.; Laird, B. B. *J. Chem. Phys.* **2006**, *125*, 094710] necessitates a re-evaluation of theoretical approaches to crystal nucleation. This has been carried out for the droplet model of the classical nucleation theory (CNT), the self-consistent classical theory (SCCT), a phenomenological diffuse interface theory (DIT), and single- and two-field variants of the phase field theory that rely on either the usual double-well and interpolation functions (PFT/S1 and PFT/S2, respectively) or on a Ginzburg–Landau expanded free energy that reflects the crystal symmetries (PFT/GL1 and PFT/GL2). We find that the PFT/GL1, PFT/GL2, and DIT models predict fairly accurately the height of the nucleation barrier known from Monte Carlo simulations in the volume fraction range of $0.52 < \phi < 0.54$, whereas the CNT, SCCT, PFT/S1, and PFT/S2 models underestimate it significantly.

1. Introduction

Nucleation of crystals in undercooled liquids is a fluctuation phenomenon, in which crystal-like embryos form that exceed the critical size determined by the interplay of the volumetric and interfacial contributions to the free energy of cluster formation.¹ Here, the free energy of the crystal–liquid interface plays a central role. However, with the exception of a few transparent systems, the experimental data are far too inaccurate to perform a conclusive test. Other uncertainties, that might limit the experimental test of nucleation theory, are the possible presence of heterogeneities and the difficulties associated with separating the nucleation prefactor from the free energy of critical clusters.^{1,2}

To date, the most reliable and most direct information on crystal nucleation is obtained from model systems. The best known simple model system that shows crystallization is the hard-sphere (HS) fluid. Extensive studies performed using the molecular dynamics (MD) and Monte Carlo (MC) techniques have clarified the main physical properties of the system:^{3–10} According to these, the fluid phase crystallizes to the fcc structure beyond the volume fraction $\phi_L = 0.492$,⁴ while the crystalline and liquid phases coexist in the volume fraction range of $0.492 < \phi < 0.543 = \phi_s$, at the coexistence pressure of $p = (11.57 \pm 0.03)kT/\sigma^3$.⁴ The equation of state (EOS) is known from atomistic simulations for a broad range of volume fractions for both the liquid^{3,5} and the crystalline phases,^{3,5} allowing one to evaluate the relative free energies of the phases, that is, the driving force of phase transition. (Critical comparison of different forms of the EOS can be found in ref 7.) One of us

has recently performed a critical assessment of the EOS for the solid and liquid phases in the range of volume fractions that are of interest from the viewpoint of freezing.⁸ It has been found that in the volume fraction range of crystallization the expressions by Hall for the fcc and a polynomial form by Tóth give the best fit to the simulation results. In contrast to the fcc phase, the bcc is known to be mechanically unstable. Specific simulation methods have been used to obtain its coexistence conditions with the liquid and its EOS.⁹ Molecular dynamics simulations have also been applied to determine the free energy of the fcc–liquid interface.¹⁰ The early results from various methods cluster around $\gamma_\infty = 0.6kT/\sigma^2$: The first evaluation of the interfacial free energy by the cleaving method yielded $\gamma_{\infty,100} = (0.62 \pm 0.01)kT/\sigma^2$, $\gamma_{\infty,110} = (0.64 \pm 0.01)kT/\sigma^2$, and $\gamma_{\infty,111} = (0.58 \pm 0.01)kT/\sigma^2$, yielding an orientation average of $\sim 0.61kT/\sigma^2$.^{10a} Comparable values have been obtained by the capillary wave technique: $\gamma_{\infty,100} = (0.64 \pm 0.02)kT/\sigma^2$; $\gamma_{\infty,110} = (0.62 \pm 0.02)kT/\sigma^2$; and $\gamma_{\infty,111} = (0.61 \pm 0.01)kT/\sigma^2$.^{10b} The interfacial free energy of small clusters has been evaluated from Monte Carlo simulations using the umbrella sampling technique yielding $(0.616 \pm 0.003)kT/\sigma^2$ for the orientation average at the large particle limit.^{10c} The free energy of small clusters has been evaluated for mono-^{10c,11a} and polydisperse^{11b} hard spheres by the same technique. It has been shown that the droplet model of the classical nucleation theory (CNT) significantly underestimates the free energy of formation of small clusters.^{11a}

These data from atomistic simulations have been used recently for validating various cluster models including the classical droplet model¹² and phase field models with intuitively chosen¹³ and with Ginzburg–Landau (GL) expanded free energy.¹² While apparently the droplet model fails for the cluster sizes in the range of simulations, other approaches including the phase field

* Corresponding author. Telephone: +36 1 392 2222Ext. 3155. Fax: +36 1 392 2221. E-mail: gytoth@szfki.hu.

theory appear to be more promising.^{12,13} Somewhat surprisingly, the GL approach, which incorporates the most detailed physical information on the system, overestimated the nucleation barrier quite substantially.¹² Recently, however, the orientational average of the interfacial free energy has been corrected downward, significantly: $\gamma_0 = 0.574kT/\sigma^2$ has been obtained by the cleaving method as a limit of the values obtained for inverse power potentials.^{10c} A recent work that addresses this question in depth, compares results from the cleaving and capillary wave methods, and revises the interfacial free energy further downward suggests that the appropriate value is $\gamma_0 = (0.56 \pm 0.02)kT/\sigma^2$.¹⁴ This $\sim 10\%$ reduction might invalidate previous conclusions drawn from the earlier value of the interfacial free energy, and necessitates a critical re-evaluation of the nucleation theories.

In this work, we have carried out a direct quantitative test for the following theoretical approaches: (i) the classical droplet model (CNT),¹⁵ (ii) the self-consistent classical theory (SCCT),¹⁶ (iii) a phenomenological diffuse interface theory (DIT),^{12,17} and a single and two-field variants of the phase field theory that rely either on the usual double-well and interpolation functions [(iv) PFT/S1¹⁸ and (v) PFT/S2,¹³ respectively] or on a Ginzburg–Landau expanded free energy that reflects the crystal symmetries [(vi) PFT/GL1^{12,18} and (vii) PFT/GL2]. This comprises the most extensive comparative study of nucleation theories for the hard-sphere system.

2. Applied Models

The models applied in the present analysis represent three different levels of abstraction:

(i) The droplet model of the classical nucleation theory (CNT): This model extends the concept of macroscopic droplets into the microscopic regime without correction, and relies on a macroscopic interfacial free energy, while assuming bulk crystal properties in the volume of the droplet. This approach is widely used in interpreting the experiments, though it is known to be of very limited accuracy at the small size of nuclei relevant for typical time scales.¹¹

(ii) Phenomenological cluster models: Two significantly different approaches are considered here. The self-consistent classical theory tries to remove the evident inconsistency of the CNT that it distinguishes the monomer of the new phase and the monomer of the parent phase, which should be, in principle, the same physical object. (It is easy to see, e.g., for vapor condensation, a single molecule “droplet” floating in the vapor phase and a single molecule of the vapor phase should indeed be indistinguishable.) The correction is, however, done in an ad hoc way, via subtracting the monomer free energy from the free energy of all cluster sizes. Still in the case of homogeneous vapor condensation, improved agreement between theory and experiment could be observed. In contrast, the phenomenological diffuse interface theory (DIT) tries to improve the droplet model via taking into account the fact that according to atomistic simulations the solid–liquid and vapor–liquid interfaces extend to several molecular layers. Assuming yet bulk crystal properties at the center of the nuclei, this approach predicts a curvature dependent interfacial free energy and usually improves significantly the agreement between theory and experiment for both vapor condensation and crystal nucleation.

(iii) Field theoretical models: These models are descendants of the van der Waals/Cahn–Hilliard/Landau type classical field theoretical models, in which the spatial change of the order parameter is penalized by a square-gradient term and has a double-well free energy density, whose minima represent the newly forming and the parent phase. Accordingly, they predict

a diffuse interface and are inherently capable of describing both small clusters composed entirely of interface and the curvature dependence of the interfacial free energy. Their accuracy, however, should depend critically on the accuracy of the double-well free energy used in the model. In this work, we are going to investigate several possible formulations.

Next, we briefly review the free energy these models predict for the critical fluctuations (nuclei). Since some of these expressions have a fairly lengthy derivation, we recall only the most important features. For details, the interested reader may refer to the original publications referenced herein.

Classical Nucleation Theory (CNT). In the droplet model of classical nucleation theory, the interface is assumed to be mathematically sharp, and the free energy of small clusters is expressed in terms of bulk and interfacial contributions yielding

$$W_{\text{CNT}} = (16\pi/3)\gamma_\infty^3/\Delta\omega^2 \quad (1)$$

for the free energy of the critical fluctuation, where $\Delta\omega$ is the volumetric grand (Landau) potential difference between the solid and liquid states (see e.g. ref 15).

Self-Consistent Classical Theory (SCCT). This approach corrects for the nonzero free energy of formation of monomers the classical droplet model predicts (a nonphysical feature¹⁶) by subtracting the monomer free energy, $W_{\text{CNT},1}$, from the classical cluster free energy:

$$W_{\text{SCCT}} = W_{\text{CNT}} - W_{\text{CNT},1} \quad (2)$$

(for details, see ref 16).

Diffuse Interface Theory (DIT). This phenomenological theory relies on the assumptions that bulk properties exist at least at the center of critical fluctuations and that the distance of surfaces of zero excess enthalpy and entropy is independent of cluster size.³⁴ The height of the nucleation barrier is given by

$$W_{\text{DIT}} = (4\pi/3)\delta_{\text{DIT}}^3\Delta\omega\psi \quad (3)$$

where $\delta_{\text{DIT}} = \gamma_\infty v/\Delta H_f$ is the characteristic interface thickness (usually a small fraction of the full interface thickness), v is the molar volume, $\Delta H_f (>0)$ is the molar heat of fusion, $\psi = 2(1+q)\xi^{-3} - (3+2q)\xi^{-2} + \xi^{-1}$, $q = (1-\xi)^{1/2}$, and $\xi = \Delta\omega/\Delta h$, while $\Delta\omega$ and Δh are the volumetric grand potential and the respective volumetric enthalpy difference between the liquid and solid. Note that the thickness parameter δ_{DIT} as defined above is usually only a fraction of the interface thickness.¹⁷ Indeed, $\delta_{\text{DIT}} = 0.4617\sigma$ for the equilibrium solid–liquid interface of the HS system. As pointed out in ref 17c, eq 3 incorporates a curvature correction up to second order in (δ_{DIT}/R) for the interfacial free energy. Application of the DIT to the HS system is detailed in ref 12. However, we relax here the assumption that the solid and liquid phases are incompressible, made in earlier DIT computations for the HS system.¹² Accordingly, herein the driving force is calculated from the pressures corresponding to the solid and liquid densities, ρ_n and ρ_0 , respectively, that have the same chemical potential, $\mu_s(\rho_n) = \mu_l(\rho_0)$. Note that, in the HS system, the only contribution to the enthalpy is from the pressure term, and $\Delta\omega = -p_s(\rho_n) + p_0$ and $\Delta h = p_0 [1 - \rho_n/\rho_0]$, where subscripts 0 and n refer to the initial liquid and the nucleating solid (of equal chemical potentials), respectively.

Phase Field Models (PFTs). We have considered four different approaches. Following previous work, the grand (Landau) potential of the inhomogeneous system relative to the initial liquid is assumed to be a local functional of the phase field m monitoring the liquid–solid transition ($m = 0$ and 1 in the liquid and in the solid, respectively) and the volume fraction $\phi = (\pi/6)\sigma^3\rho$ (here, ρ is the number density of hard spheres):¹³

$$\Delta\Omega = \int d^3r \left\{ \frac{\varepsilon^2 T}{2} (\nabla m)^2 + \Delta\omega(m, \dots) \right\} \quad (4)$$

where ε is a coefficient that can be related to the interfacial free energy and the interface thickness, T is the temperature, while $\Delta\omega(m, \dots)$ is the local grand free energy density relative to the initial state (which, in the presence of an additional conserved field, such as ϕ or ρ , includes a Lagrange multiplier term, that ensures mass conservation; here, the Lagrange multiplier is related to the chemical potential of the initial liquid¹³). The gradient term leads to a diffuse crystal–liquid interface, a feature observed in both experiment²⁰ and computer simulations.²¹ In this work, the grand potential density is assumed to have the following two simple forms:

Skewed double-well free energy:

$$\Delta\omega(m) = wTg(m) + p(m) \left\{ f_S(\phi_n) - \frac{\partial f_L}{\partial \phi(\phi_n)} [\phi_n - \phi_\infty] - f_L(\phi_\infty) \right\} \quad (5a)$$

Free energy surface:

$$\Delta\omega(m, \phi) = wTg(m) + p(m) f_S(\phi) + [1 - p(m)] f_L(\phi) - \frac{\partial f_L}{\partial \phi(\phi_\infty)} [\phi - \phi_\infty] - f_L(\phi_\infty) \quad (5b)$$

where $f_S(\phi)$ and $f_L(\phi)$ are the Helmholtz free energy densities for the solid and liquid states, respectively, while ϕ_∞ and ϕ_n are the volume fraction of the initial liquid phase and the crystalline phase that provides the largest driving force relative to the initial liquid, respectively. Different “double-well” $g(m)$ and “interpolation” functions $p(m)$ have been used as specified below. The free energy scale w determines the height of the free energy barrier between the bulk solid and liquid states. Once the functional forms of $g(m)$ and $p(m)$ are specified, model parameters ε and w can be expressed in terms of γ_∞ and the thickness δ of the equilibrium planar interface.^{22,12,13,18}

We have used two sets of these functions. One of them has been proposed intuitively in an early formulation of the PFT²³ and is in use widely:

(a) The “standard” set (PFT/S): These functions are assumed to have the form $g(\varphi) = (1/4)\varphi^2(1 - \varphi)^2$ and $p(\varphi) = \varphi^3(10 - 15\varphi + 6\varphi^2)$ that emerge from an intuitive formulation of the PFT.²³ Here, $\varphi = 1 - m$ is the complementing phase field, defined so that it is 0 in the solid and 1 in the liquid.

(b) Ginzburg–Landau form for fcc structure (PFT/GL): Recently, we have attempted the derivation of these functions for bcc (base centered cubic) and fcc (face centered cubic) structures^{2c} on the basis of a single-order-parameter Ginzburg–Landau (GL) expansion that considers the fcc crystal symmetries. This treatment yields

$$g(m) = (1/6)(m^2 - 2m^4 + m^6) \quad (6a)$$

and

$$p(m) = 3m^4 - 2m^6 \quad (6b)$$

while the expressions that relate the model parameters to measurable quantities are as follows: $\varepsilon_{GL}^2 = (8/3)C\varepsilon_S^2$, $w_{GL} = w_S(4C)^{-1}$, where $C = \ln(0.9/0.1)[3\ln(0.9/0.1) - \ln(1.9/1.1)]^{-1}$. This model has been denoted as PFT/GL1 when used with eq 5a and PFT/GL2 when combined with eq 5b. The former can be obtained as the single component limit of the binary PFT/GL of ref 18, while the latter is a new construction presented here the first time. Therefore, though it is similar to the procedure followed before,¹³ it is appropriate to briefly outline the way the properties of the nucleus are determined:

Being in unstable equilibrium, the critical fluctuation (the nucleus) can be found as an extremum (saddle point) of the grand free energy.^{22,12,13,18,19} The field distributions, that extremize the free energy, can be obtained solving the appropriate Euler–Lagrange (EL) equations.^{22,12,13,18,19}

$$\frac{\delta\Omega}{\delta m} = \frac{\partial I}{\partial m} - \nabla \cdot \frac{\partial I}{\partial \nabla m} = 0 \quad (7a)$$

and

$$\frac{\delta\Omega}{\delta \phi} = \frac{\partial I}{\partial \phi} - \nabla \cdot \frac{\partial I}{\partial \nabla \phi} = 0 \quad (7b)$$

where $\delta\Omega/\delta m$ and $\delta\Omega/\delta\phi$ stand for the first functional derivative of the grand free energy with respect to the fields m and ϕ . Here, $I = 1/2\varepsilon^2 T(\nabla m)^2 + \Delta\omega(m, \phi)$ is the total grand free energy density of the system. For the sake of simplicity, an isotropic interfacial free energy (a reasonable approximation for simple liquids) is assumed. Note that, due to a lack of a gradient term for the field ϕ , eq 7b yields an implicit relationship between m and ϕ , which can be then inserted into eq 7a, when solving it.

Assuming an unperturbed liquid ($m = 0$, $\phi = \phi_\infty$) in the far field ($r \rightarrow \infty$) and, for symmetry reasons, a zero field gradient at the center of the fluctuations, m and dm/dr are fixed at different spatial locations. Therefore, in this work, eq 7a has been solved numerically, using a *relaxation* method²⁴ suitable for handling such two-point boundary value problems. Having determined the solutions $m(r)$ and $\phi(r)$, the work of formation of the nucleus, W^* , has been obtained by inserting these solutions into the grand potential functional eq 4.

Of all these phase field models, the latter two (PFT/GL1 and PFT/GL2), which rely on the Ginzburg–Landau expansion, incorporate the most detailed physical information on the system (e.g., crystal structure); therefore, they are expected to provide the best approximation to the atomistic simulations.

For all models, we have applied the following test: First, we fix the model parameters in equilibrium, and then we predict the nucleation barrier in the supersaturated state without any adjustable parameters, and this is then compared to accurate data from MC simulation.

3. Thermodynamic Properties

In the computations, if not stated otherwise, we have used the equations of state Hall obtained for the solid and liquid states²⁵ by fitting to the molecular dynamics simulation results of Alder and Wainwright.⁵ For comparison, we performed a few calculations with a polynomial equation of state for the high-density liquid by Tóth,⁸ which has been fitted to the data from MD simulations (Figure 1):

$$Z(\phi) = \left\{ (\phi - \phi_g) \sum_{i=0}^6 c_i (\phi - \phi_g)^i \right\}^{-1} \quad (8)$$

where $Z = p/(\rho kT)$ is the compressibility factor, $\phi_g = 0.63885$, $c_0 = -0.8187$, $c_1 = -3.889$, $c_2 = -17.407$, $c_3 = -20.503$, $c_4 = 12.649$, $c_5 = 60.336$, and $c_6 = 41.859$. We use a recently revised value for the interfacial free energy $\gamma_0 = (0.56 \pm 0.02)kT/\sigma^2$,¹⁴ while the 10%–90% interface thickness is allowed to change in the range of $d_{10\%-90\%} = (3.15 \pm 0.15)\sigma$. We note that, in a previous study, substantially larger interface thicknesses (4.75σ to 5.94σ) have been used, evaluated from the envelope of the density peaks.¹³ Our present choice is probably more reliable, as it is consistent with interfacial profiles obtained for a variety of structure-related physical properties such as coarse grained density, diffusion, and the orientational order parameters q_4 and q_6 at the equilibrium solid–liquid interface of the hard-sphere system.⁶ It is worth mentioning that the interfacial data from atomistic simulations might underestimate both the interfacial free energy and the interface thickness due to the limited size of such simulations, which leads to a long wavelength cutoff in the spectrum of surface fluctuations. Nevertheless, the surface areas typical for nuclei and for the equilibrium solid–liquid interface used in atomistic simulations are roughly comparable, so only minor errors are expected from this source.

4. Results and Discussion

The predictions for the structure of the critical fluctuations are presented in Figure 2 for the three initial volume fractions ($\phi_L = 0.5207$, 0.5277 , and 0.5343) Auer and Frenkel used in their atomistic simulations.¹¹ For the CNT, SCCT, and DIT, the solid–liquid structural order parameter is shown to change from 1 to 0 as a step function at the predicted radius of the surface of tension,²⁶ defined by the expression [see, e.g., ref 18 or 27]

$$R_p = \left(\frac{3W^*}{2\pi\Delta\omega} \right)^{1/3} \quad (9)$$

where $\Delta\omega$ is the driving force of crystallization (grand potential difference between the bulk liquid and solid phases).

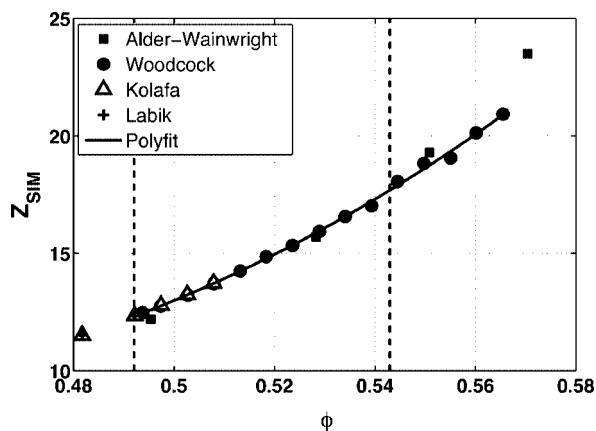


Figure 1. Equation of state for the solid state (compressibility factor versus volume fraction). Results from atomistic simulations⁵ are shown together with the polynomial fit (solid line) to the most detailed data set by Woodcock⁵ (full circles). Note the reasonable agreement among simulation data obtained by different authors. The vertical dashed lines show the volume liquid and solid phases coexisting at $p = 11.57kT/\sigma^3$.

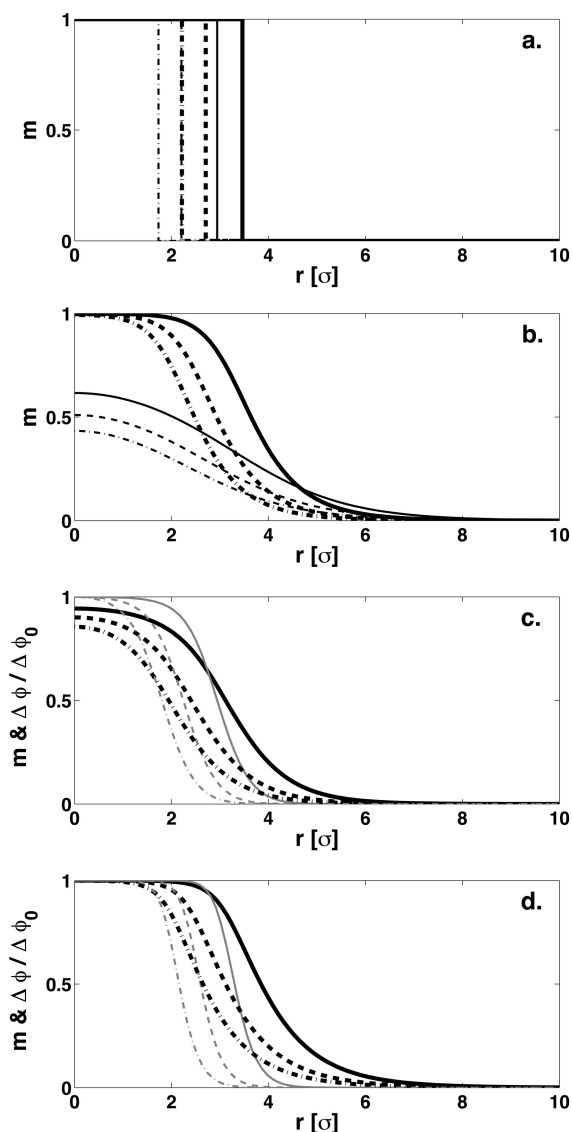


Figure 2. Structure of the critical fluctuations as predicted by various cluster models at three initial liquid volume fractions (0.5207 , 0.5277 , and 0.5343 , denoted by solid, dashed, and dash-dotted lines, respectively; a sequence corresponding to decreasing size): (a) solid–liquid structural order parameter for the CNT and SCCT (heavy lines, coinciding for the two models) and for the DIT (light lines); (b) for the single-order-parameter phase field models, PFT/GL1 (heavy lines) and PFT/S1 (light lines); (c) structural order parameter profiles (heavy lines) and normalized fractional density difference (light lines) profiles for PFT/S2; and (d) the same for PFT/GL2. Note the similarity of the solutions from PFT/S1 and PFT/S2, and also the solutions from PFT/GL1 and PFT/GL2.

The size of nuclei falls into the $\sim 2\sigma$ to 4σ range in all the theoretical predictions, with the latter corresponding to the smallest driving force ($\phi_L = 0.5207$). Remarkably, this is in reasonable agreement with the snapshot of the respective nucleus from the MC simulation (Figure 3 of ref 11a). In this size range, however, the radius of the nuclei is comparable to the thickness of the interface. Accordingly, the sharp interface approaches (CNT and SCCT) are expected to be of limited accuracy.

We note the asymmetry of the structural order parameter profiles from the phase field computations with Ginzburg–Landau expanded free energies: sharper on the solid side and more gradual on the liquid side. This is in agreement with the predictions from our previous work^{11,18} for fcc structure and with a full molecular theory by Shen and Oxtoby.^{19c} Interest-

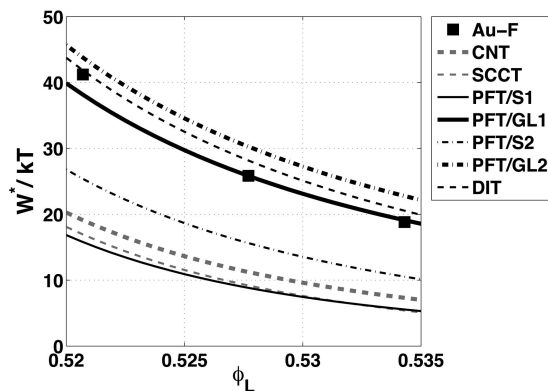


Figure 3. Nucleation barrier W^* measured in kT units versus initial volume fraction of the liquid phase (ϕ_L) as predicted by various cluster models: CNT, droplet model of the classical nucleation theory; SCCT, self-consistent classical theory; PFT/S1, single order parameter phase field theory with the standard double-well and interpolation functions; PFT/GL1, single order parameter phase field theory with Ginzburg–Landau free energy; PFT/S2, with the standard double-well and interpolation functions, structural order parameter, and density field; PFT/GL2, as PFT/S2, however, with double-well and interpolation functions from Ginzburg–Landau expansion; and DIT, phenomenological diffuse interface theory. For comparison, the nucleation barrier height from direct atomistic (MC) simulations of Auer and Frenkel¹¹ (Au–F) are also shown. Note that the uncertainty of W^* from atomistic simulation is about $\pm 1.5kT$ (see Figure 1 of ref 11a), roughly corresponding to the size of the symbol used here.

ingly, the solutions from the PFT/GL1 and PFT/GL2 models are rather similar, as are those from the PFT/S1 and PFT/S2 models, with the latter showing a significant deviation from the bulk crystal properties even at the center of the nuclei.

The respective nucleation barrier heights are compared to the results of Monte Carlo simulations in Figure 3. We find that, without adjustable parameters, in the investigated volume fraction range, the predictions of the PFT/GL1, PFT/GL2, and DIT models are in a reasonable agreement with highly accurate results from atomistic simulations. In contrast, the other models (CNT, SCCT, PFT/S1, and PFT/S2) considerably underestimate the height of the nucleation barrier. The present failure of the droplet model of the CNT in predicting the free energy of small clusters is not surprising and is in accord with earlier results for the HS^{10c,11} and other systems, including ice–water,^{19d,g} Ag–Cu,¹⁸ and NaCl.²⁸ It is nevertheless remarkable that, unlike the case of vapor condensation,¹⁶ the *self-consistency correction changes the nucleation barrier in the wrong direction*. It is reassuring that, by incorporating more physical details (such as crystal symmetries) into continuum theory, there is improved agreement with the atomistic simulations.

Next, we estimate the effect of the error of the input parameters on the nucleation barrier computed using PFT/GL1. Using the lower and upper limits allowed by the expressions $\gamma_0 = (0.56 \pm 0.02)kT/\sigma^2$ and $d_{10\%-90\%} = (3.15 \pm 0.15)\sigma$ leads to only minor changes in the height of the nucleation barrier (see Figure 4), which do not influence the conclusions in any significant way. Similarly, the uncertainties emerging from the error of the equilibrium pressure and the equations of state are also negligible.

It is also appropriate to assess how far these results are influenced by the anisotropy of the solid–liquid interfacial free energy. In the case of the continuum models, this will require the solution of the Euler–Lagrange equations in 3D, by adopting numerical methods recently applied for the analogous problem of solid-state nucleation.²⁹ However, a less demanding computa-

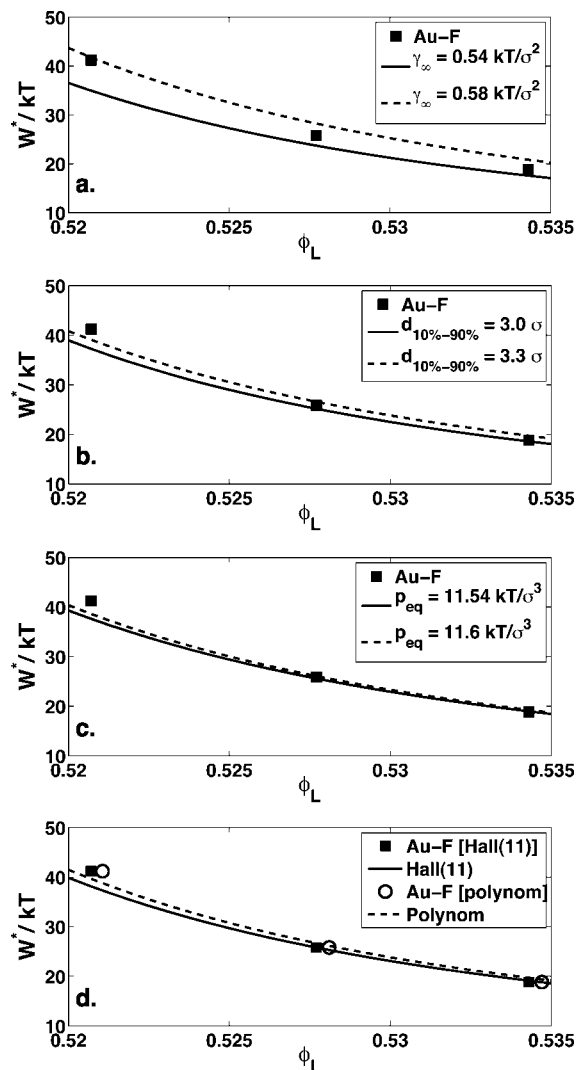


Figure 4. Sensitivity of the nucleation barrier (predicted by PFT/GL1) to the uncertainty of (a) the interfacial free energy, (b) the interface thickness, (c) the equilibrium pressure, and (d) the equation of state for the liquid phase [here, (11) refers to eq 11 of Hall⁵]. For comparison, the Monte Carlo simulations of Auer and Frenkel^{11a} (Au–F) are also shown [in panel (d), empty circles stand for MC results with volume fractions corresponding to the polynomial equation of state eq 8, as opposed to the full squares whose volume fraction coordinates have been computed using eq 11 of Hall⁵]. Note that the main source of uncertainty to the nucleation barrier can be identified as the uncertainty of the interfacial free energy.

tion can be made in the case of the comparably accurate DIT.^{17b,30} Being in an unstable equilibrium, the enthalpy and entropy surfaces of the nucleus (as defined in the DIT) have the equilibrium shape, and the nucleation barrier can be computed by replacing the volume of the unit sphere in eq 3 by the volume of the equilibrium shape normalized with the volume of the sphere corresponding to the orientation averaged interfacial free energy, where the anisotropy of the interfacial free energy of the solid–liquid interface is given by the Kubic harmonic expansion of Fehlner and Vosko,³¹

$$\gamma(\mathbf{n})/\gamma_0 = 1 + \varepsilon_1 \left(\sum_{i=1}^3 n_i^4 - \frac{3}{5} \right) + \varepsilon_2 \left(\sum_{i=1}^3 n_i^4 + 66n_1^2 n_2^2 n_3^2 - \frac{17}{7} \right) \quad (10)$$

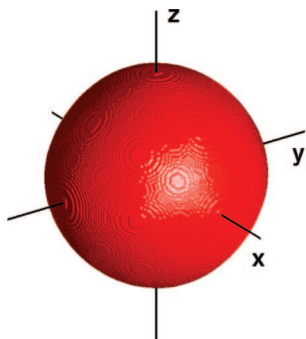


Figure 5. Equilibrium crystal shape (Wulff shape³²) corresponding to the anisotropy function given by eq 10. Note the close to spherical form.

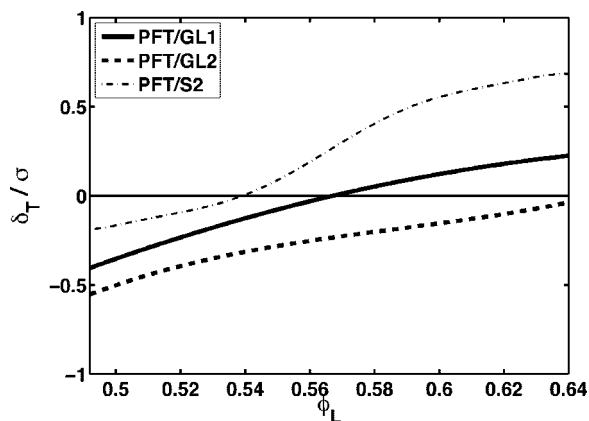


Figure 6. Tolman length predicted by various phase field models as a function of the volume fraction of the initial (supersaturated) liquid state.

where the recently revised parameter set,¹⁴ $\gamma_0 = 0.559(17)kT/\sigma^2$, $\varepsilon_1 = 0.072(9)$, and $\varepsilon_2 = -0.004(2)$, has been used. The equilibrium shape has been computed following the Wulff construction,³² and it is shown in Figure 5. The anisotropy is small, and the respective correction to the nucleation barrier is less than 1%: $W_{\text{DIT}}^{\text{aniso}} \cong (1.009 \pm 0.001)W_{\text{DIT}}^{\text{iso}}$, a result that does not influence the conclusions drawn from the computations performed with an isotropic interfacial free energy in any significant way.

The present phase field computations offer a unique possibility to derive the magnitude of the Tolman length,³³ δ_T , a parameter introduced some time ago to capture the curvature dependence of the interfacial free energy, and has been evaluated for the crystal–liquid interface from atomistic simulations for the Lennard–Jones system.³⁴ It is defined as the difference of the radii of the equimolar surface³⁵ and the surface of tension:²⁶ $\delta_T = R_e - R_p$. The evaluation of these quantities is straightforward for the PFT/S2 and PFT/GL2 models, where the spatial variation of the number density is explicitly calculated. In the case of the PFT/GL1 model, where we have a single (structural) order parameter, we have chosen the following approach: As pointed out by Shih et al.,³⁶ in the Ginzburg–Landau expansion the PFT/GL1 model is based on, the fractional density change is expected to be proportional to m^2 . Thus, the radius of the equimolar surface can be obtained from the solution of the EL equation as $R_e = [\int 4\pi r^2 m^2(r) dr / (4\pi/3)]^{1/3}$.

The results for the Tolman length are shown as a function of initial volume fraction in Figure 6. For the PFT/S2 and PFT/GL1 models, a positive value is observed at high supersaturations, which continuously decreases toward the negative equi-

librium values. This behavior is consistent with earlier field theoretic results^{27,38} and atomistic simulations.³⁴ In contrast, for PFT/GL2, we have observed a negative Tolman length over the whole range of volume fractions investigated. It is appropriate to mention that, in the high density region ($\phi > 0.58$), the Tolman length is extremely sensitive to the choice of the equation of state of the liquid, especially in the vicinity of the dense random packed limit, where the equations of state from different sources may differ significantly.^{5,38} For example, for PFT/S2 and PFT/GL2, we were unable to solve the EL equations with the EOS given by eq 8 above $\phi > 0.58$, despite the fact that eq 8 gives indeed an excellent fit to simulation data for the high density fluid. Such difficulty does not occur for Hall's EOS. At this stage, it is unclear whether a more accurate EOS would mitigate this problem, or it is the phenomenological definition of the free energy surface (eq 5b) that is responsible for the absence of the solutions of the PFT/S2 and PFT/GL2 models at high fluid densities. Work is underway to investigate this question.

We wish to mention here that a Ginzburg–Landau free energy functional has recently been constructed for the HS system relying on the fundamental measure approach to the density functional theory (DFT-FM), and it has been used to investigate the liquid–fcc interface and the nucleation barrier.⁴⁰ This approach has the advantage that it *predicts* the interfacial properties of the liquid–fcc interface, whereas the far simpler continuum models used in the present paper need the interfacial properties as an input. Unfortunately, while the interfacial free energies, $0.69kT/\sigma^2$ and $0.66kT/\sigma^2$, the two variants of the DFT-FM⁴⁰ predicted for the equilibrium crystal–fluid interface, are fairly accurate for approaches based on first principles, these values significantly exceed the best value $(0.56 \pm 0.02)kT/\sigma^2$ from atomistic simulations. Accordingly, a direct comparison of the DFT-MF results with our predictions for the nucleation barrier (obtained with accurate interfacial data) or with the respective MC results might prove inconclusive.

At this point, we wish to comment on the possible relevance of our results to nucleation experiments, including those on colloidal systems that mimic the hard-sphere interaction.^{41,42} Besides light scattering experiments,^{41,42} laser scanning confocal microscopy used in some of the colloidal nucleation experiments proved a truly powerful technique.⁴² It is able to follow the trajectory of the individual colloidal particles, and in this sense it is an experimental counterpart of the MD simulations: nucleation can be followed in real time.⁴² Interestingly, the agreement between nucleation rates from experiments on colloidal systems and from computer simulations with the exact HS potential is not particularly good.^{11a} A possible explanation is that, due to some remnant charges, the interaction is not yet the exact HS interaction. This view is supported by the fact that some of these colloidal systems used in the experiments crystallize at volume fractions where the true HS system should not [e.g., the coexistence region is $0.38 < \phi < 0.42$ (ref 44) as opposed to $0.492 < \phi < 0.543$ for the HS system]. As a result, neither the HS equations of state nor the HS interfacial free energy data seems to be applicable. Without this information, however, one falls back to the usual situation: the nucleation rate can be measured, but then one needs a kinetic theory that defines the pre-exponential factor of nucleation, J_0 ,⁴³ to evaluate the free energy of nuclei, and then again a cluster model is required to evaluate the interfacial free energy. The accuracy of the interfacial free energy determined so critically depends on the accuracy of both the pre-exponential factor and the cluster model. We note that even if J_0 is known with some accuracy⁴³

and the experiments indeed refer to homogeneous nucleation,⁴³ such experiments may only be used to validate nucleation theories, if the interfacial free energy is available with a sufficient accuracy from an independent source (however, such information is usually unavailable). This situation makes the present quantitative test of nucleation theory on the HS system indeed unique. A similar test could be performed for other systems after extending the atomistic simulations to obtain the EOS, the interfacial free energy, and the free energy of nuclei. Possible candidates are the Lennard–Jones fluid and some metals (whose interatomic interaction is approximated by the embedded atom potential), as the required information is partially available for them.

We mention finally that a straightforward utilization of the present results could be to combine the advanced cluster models (DIT, PFT/GL1, or PFT/GL2) validated here with cluster dynamics computations to improve the quality of interfacial free energy data extracted from nucleation rate measurements, as done previously using the Cahn–Hilliard model.⁴⁴ Although our results refer strictly to hard spheres, many of the monatomic liquids, including the Lennard–Jones system and the metals, display features close to those of the HS system,⁴⁵ implying that the present results are probably relevant to a broader range of systems.

5. Summary

A quantitative test of nucleation theories has been performed for the hard-sphere systems with the recently updated value of the solid–liquid interfacial free energy. It has been found that, after fixing all model parameters using the equilibrium properties of the solid–liquid interface, the phase field models with Ginzburg–Landau free energy (PFT/GL1 and PFT/GL2) and a phenomenological diffuse interface theory (DIT) predict fairly accurately the height of the nucleation barrier. In contrast, phase field models using the standard double-well and interpolation functions (PFT/S1 and PFT/S2) significantly underestimate the nucleation barrier. Similar behavior is observed for sharp interface models, such as the droplet model of the classical nucleation theory (CNT) and the self-consistent classical theory (SCCT).

Acknowledgment. This work has been supported by the Hungarian Academy of Sciences under Contract No. OTKA-K-62588. We are indebted to László Környei (Res. Inst. Solid State Physics and Optics, Budapest, Hungary) for his help in constructing/visualizing the Wulff shape and to Geoffrey Scamans (BCAST, Brunel University, U.K.) for his critical reading of the manuscript.

References and Notes

- (1) For reviews on crystal nucleation, see (a) Kelton, K. F. *Solid State Phys.* **1991**, *45*, 75; (b) Wu, D. T.; Gránásy, L.; Spaepen, F. *MRS Bull.* **2004**, *29*, 945.
- (2) (a) Kelton, K. F.; Greer, A. L. *Phys. Rev. B* **1988**, *38*, 10089. (b) Kelton, K. F.; Greer, A. L. *J. Am. Ceram. Soc.* **1991**, *75*, 1015. (c) ten Wolde, P. R.; Ruiz-Montero, M. J.; Frenkel, D. *J. Chem. Phys.* **1996**, *104*, 9932.
- (3) Hoover, W. G.; Ree, F. H. *J. Chem. Phys.* **1969**, *49*, 3609.
- (4) Davidchack, R. L.; Laird, B. B. Personal communication, 2004.
- (5) Atomistic simulations for HS system: Alder, B. J.; Wainwright, T. E. *J. Chem. Phys.* **1960**, *33*, 1439, ref 3. Woodcock, L. V. *J. Chem. Soc., Faraday Discuss.* **1976**, *72*, 731. Erpenbeck, J. J.; Wood, W. W. *J. Stat. Phys.* **1984**, *35*, 321. Barosova, M.; Kolafa, J. Reported in ref 7. Equations of state for fluid: Carnahan, N. F.; Starling, K. E. *J. Chem. Phys.* **1969**, *51*, 635. Hall, K. R. *J. Chem. Phys.* **1972**, *57*, 2252. Le Fevre, E. *J. Nature (London)* **1972**, *325*, 20. Andrews, F. C. *J. Chem. Phys.* **1975**, *62*, 272. Baus, M.; Colot, J. L. *Phys. Rev. A* **1987**, *36*, 3912. Maeso, M. J.; Solana, J. R.; Amorós, J.; Villar, E. *J. Chem. Phys.* **1991**, *94*, 551. Sanchez, I. C. *J. Chem. Phys.* **1994**, *101*, 7003. Wang, W.; Khoshkbarchi, M. K.; Vera, J. H. *Fluid Phase Equilib.* **1996**, *115*, 25. Malijevsky, A.; Veverka, J. *Phys. Chem. Chem. Phys.* **1999**, *1*, 4267. Kolafa, J.; Labik, S.; Malijevsky, A. *Phys. Chem. Chem. Phys.* **2004**, *6*, 2335. Equations of state for fcc crystal: Hall, K. R. *J. Chem. Phys.* **1972**, *57*, 2252. Speedy, R. J. *J. Phys.: Condens. Matter* **1998**, *10*, 4387. Chang, J.; Sandler, S. I. *J. Chem. Phys.* **2003**, *118*, 8390.
- (6) Davidchack, R. L.; Laird, B. B. *J. Chem. Phys.* **1998**, *108*, 9452.
- (7) Mulero, A.; Galan, C.; Cuadros, F. *Phys. Chem. Chem. Phys.* **2001**, *1*, 4991.
- (8) Tóth, G. I. Diploma Thesis, Technical University Budapest, Hungary, 2004.
- (9) Woodcock, L. V. *Faraday Discuss.* **1997**, *106*, 325.
- (10) (a) Davidchack, R. L.; Laird, B. B. *Phys. Rev. Lett.* **2000**, *85*, 4751. (b) Davidchack, R. L.; Laird, B. B. *J. Phys. Chem. B* **2005**, *109*, 17802. (c) Cacciuto, A.; Auer, S.; Frenkel, D. *J. Chem. Phys.* **2003**, *119*, 7467.
- (11) (a) Auer, S.; Frenkel, D. *Nature* **2001**, *409*, 1020. (b) Auer, S.; Frenkel, D. *Nature* **2001**, *413*, 711.
- (12) Gránásy, L.; Pusztai, T. *J. Chem. Phys.* **2002**, *117*, 10121.
- (13) Gránásy, L.; Pusztai, T.; Tóth, G.; Jurek, Z.; Conti, M.; Kvamme, B. *J. Chem. Phys.* **2003**, *119*, 10376.
- (14) Davidchack, R. L.; Morris, J. R.; Laird, B. B. *J. Chem. Phys.* **2006**, *125*, 094710.
- (15) Farkas, L. *Z. Phys. Chem. (Lepzig) A* **1935**, *125*, 236. Becker, R.; Döring, W. *Ann. Phys. (Paris, Fr.)* **1935**, *24*, 719. Turnbull, D.; Fisher, J. *C. J. Chem. Phys.* **1949**, *17*, 71.
- (16) Girshick, S. L.; Chiu, C. P. *J. Chem. Phys.* **1990**, *93*, 1273. Girshick, S. L. *J. Chem. Phys.* **1991**, *94*, 826.
- (17) (a) Gránásy, L. *Europhys. Lett.* **1993**, *24*, 121. (b) Gránásy, L. *J. Phys. Chem.* **1995**, *99*, 14182. (c) Gránásy, L. *J. Chem. Phys.* **1996**, *104*, 5188. (d) Gránásy, L.; Iglói, F. *J. Chem. Phys.* **1997**, *107*, 3634. (e) Gránásy, L. *J. Non-Cryst. Solids* **1997**, *219*, 49.
- (18) Tóth, G. I.; Gránásy, L. *J. Chem. Phys.* **2007**, *127*, 074709; 074710; PFT/S1—single component limit of binary PFT/S used in these papers; PFT/GL1—single component limit of binary PFT/GL.
- (19) Continuum models of crystal nucleation: (a) Oxtoby, D. W. In *Liquids, Freezing and Glass Transition*; eds. Hansen, J. P., Lesvesque, D., Zinn-Justin, J., Eds.; Elsevier: Amsterdam, 1991; p 145. (b) Oxtoby, D. W. *J. Phys.: Condens. Matter* **1992**, *4*, 7627. (c) Shen, Y. C.; Oxtoby, D. W. *J. Chem. Phys.* **1996**, *104*, 4233; **1996**, *105*, 2130. (d) Gránásy, L. *J. Mol. Struct.* **1999**, *485–486*, 523. (e) Gránásy, L.; Oxtoby, D. W. *J. Chem. Phys.* **2000**, *112*, 2399. (f) Oxtoby, D. W. *Annu. Rev. Mater. Res.* **2002**, *32*, 39. (g) Gránásy, L.; Börzsönyi, T.; Pusztai, T. *Phys. Rev. Lett.* **2002**, *88*, 206105.
- (20) For example, Broughton, J. Q.; Gilmer, G. H. *J. Chem. Phys.* **1986**, *84*, 5749; Laird, B. B.; Haymet, A. D. *J. Chem. Phys.* **1992**, *92*, 1819; Sibug-Aga, R.; Laird, B. B. *Phys. Rev. B* **2002**, *66*, 144106; Ramalingam, H.; Asta, M.; van der Walle, A.; Hoyt, J. J. *Interface Sci.* **2002**, *10*, 149.
- (21) Howe, J. M. *Philos. Mag. A* **1996**, *74*, 761. Schumacher, P.; Greer, A. L. In *Light Metals*; Hale, W., Ed.; The Minerals, Metals, and Materials Society: Warrendale, PA, 1996; p 745. Huisman, W. J.; Peters, J. F.; Zwanenburg, M. J.; de Wries, S. A.; Derry, T. E.; Abernathy, D.; van der Veen, J. F. *Nature* **1997**, *390*, 379. Howe, J. M.; Saka, H. *MRS Bull.* **2004**, *29*, 951. van der Veen, J. F.; Reichert, H. *MRS Bull.* **2004**, *29*, 958.
- (22) Cahn, J. W.; Hilliard, J. E. *J. Chem. Phys.* **1958**, *28*, 258; **1959**, *31*, 688. Warren, J. A.; Boettinger, W. J. *Acta Metall. Mater.* **1995**, *43*, 689.
- (23) Wang, S. L.; Sekerka, R. F.; Wheeler, A. A.; Murray, B. T.; Coriell, S. R.; Braun, R. J.; McFadden, G. B. *Phys. D* **1993**, *69*, 189.
- (24) Press, W. H.; Teukolsky, S. A.; Wetterling, W. T.; Flannery, B. P. *Numerical Recipes in C*; Cambridge University Press: Cambridge, UK, 1992; Chapter 17.3.
- (25) Equations of state by K. R. Hall (*J. Chem. Phys.* **1972**, *57*, 2252): fluid phase, eq 11; solid phase, eq 13.
- (26) The surface of tension is the surface at which the surface tension acts. It is the surface for which the generalized Laplace equation, $\Delta p_c = 2\gamma/R + \partial\gamma/\partial R$ reduces to the original one, that is, $\partial\gamma/\partial R = 0$. Here, Δp_c is the capillary pressure.
- (27) Koga, K.; Zeng, X. C.; Shcheekin, A. X. *J. Chem. Phys.* **1998**, *109*, 4063.
- (28) Zykova-Timan, T.; Valeriani, C.; Sanz, E.; Frenkel, D.; Tosatti, E. *Phys. Rev. Lett.* **2008**, *100*, 036103.
- (29) Zhang, L.; Chen, L. Q.; Du, Q. *Phys. Rev. Lett.* **2007**, *98*, 265703.
- (30) Gránásy, L.; Pusztai, T.; Hartmann, E. *J. Cryst. Growth* **1996**, *167*, 756.
- (31) Fehlner, W. R.; Vosko, S. H. *Can. J. Phys.* **1976**, *54*, 2159.
- (32) For example, Kobayashi, R.; Giga, Y. *Jpn. J. Ind. Appl. Math.* **2001**, *18*, 207.
- (33) Tolman's original definition (Tolman, R. C. *J. Chem. Phys.* **1949**, *17*, 333). A different definition is applied by several authors: $\delta_T = \lim_{R \rightarrow \infty} R_c - R_p$. In our terminology, the latter corresponds to the equilibrium Tolman length, $\delta_{T,eq}$.
- (34) Báez, L. A.; Clancy, P. *J. Chem. Phys.* **1995**, *102*, 8138.

(35) Defined by the position of a step function that has the same spatial integral and amplitude as the interfacial density profile.

(36) Shih, W. H.; Wang, Z. Q.; Zeng, X. C.; Stroud, D. *Phys. Rev. A* **1987**, *35*, 2611.

(37) Field theoretic models of the vapor–liquid interface predict a strongly size dependent Tolman length that has a positive value for small droplets and tends to a negative value in the large particle limit. See, for example, Fisher, M. P. A.; Wortis, M. *Phys. Rev. B* **1984**, *29*, 625. Iwamatsu, M. *J. Phys.: Condens. Matter* **1994**, *6*, L173. Hadjiagapiou, I. *J. Phys.: Condens. Matter* **1994**, *6*, 5303. Talanquer, V.; Oxtoby, D. W. *J. Phys. Chem.* **1995**, *99*, 2865. van Giessen, A. E.; Blokhuis, E. M.; Bukman, D. *J. J. Chem. Phys.* **1998**, *108*, 1148. Gránásy, L. *J. Chem. Phys.* **1998**, *109*, 9660. Barrett, J. *J. Chem. Phys.* **1999**, *111*, 5938. Barrett, J. C. *J. Chem. Phys.* **2006**, *127*, 144705. Hruby, J.; Labetski, D. G.; van Dongen, M. E. H. *J. Chem. Phys.* **2007**, *127*, 164720.

(38) Goldman, J. I.; White, J. A. *J. Chem. Phys.* **1988**, *89*, 6403. Speedy, R. J. *J. Chem. Phys.* **1994**, *100*, 6684. Sanchez, I. C. *J. Chem. Phys.* **1994**, *101*, 7003. Rintoul, M. D.; Torquato, S. *J. Chem. Phys.* **1996**, *105*, 9258. Gruhn, T.; Monson, P. A. *Phys. Rev. E* **2001**, *64*, 061703. Wu, G.-W.; Sados, R. J. *AIChE J.* **2005**, *51*, 309.

(39) Lutsko, J. F. *Phys. Rev. E* **2006**, *74*, 021603.

(40) Rosenfeld, Y.; Schmidt, M.; Lowen, H.; Tarazona, P. *Phys. Rev. E* **1997**, *55*, 4245. Tarazona, P. *Phys. A* **2002**, *306*, 243.

(41) Schatzel, K.; Ackerson, B. J. *Phys. Rev. E* **1993**, *48*, 3766. Harland, J. L.; van Meegen, W. *Phys. Rev. E* **1997**, *55*, 3054. Palberg, T. *J. Phys.: Condens. Matter* **1999**, *11*, R323. Sinn, C.; Heymann, A.; Stipp, A.; Palberg, T. *Trends Colloid Interface Sci.* **2001**, *118*, 266.

(42) Gasser, U.; Weeks, E. R.; Schofield, A.; Pusey, P. N.; Weitz, D. A. *Science* **2001**, *292*, 258.

(43) Nucleation theories predict the expression $J = J_0 \exp\{-W^*/kT\}$ for the steady-state nucleation rate,^{2a} where J_0 is the pre-exponential factor depending on the molecular mobility and the size of the critical fluctuation, while W^* is the free energy of the critical fluctuation (nucleus). Experimental

studies imply that J_0 from the kinetic approach of the CNT describes properly the temperature dependence of the nucleation rate.^{2a,b} Langer's first principles approach offers an independent way to estimate J_0 [Langer, J. S. *Ann. Phys. (N.Y.)* **1967**, *41*, 108; **1969**, *54*, 258]. In the few cases where J_0 has been evaluated following this route (e.g., for vapor condensation: Langer, J. S.; Turski, L. A. *Phys. Rev. A* **1973**, *8*, 3230), it leads to results very close to those from the classical kinetic approach. For crystal nucleation, Langer's approach has only been used to evaluate J_0 under the assumption that thermal transport is the rate determining factor (Grant, M.; Gunton, J. D. *Phys. Rev. B* **1985**, *32*, 7300). However, usually this is not the case, as normally molecular mobility determines the time scale of nucleation.^{2a} Atomistic simulations imply that for the Lennard–Jones system J_0 from the classical kinetic approach might be too low by about 2 orders of magnitude.^{2c} This indicates that some uncertainty has to be associated with the nucleation barrier if evaluated from the measured nucleation rates using the classical J_0 .^{2a} A further difficulty is that often steady state nucleation is assumed when evaluating the experiments without testing whether this assumption is valid. An even more essential source of error can be the presence of heterogeneous nucleation induced by foreign particles distributed in the volume. It cannot be easily distinguished from homogeneous nucleation, and the interpretation of heterogeneous nucleation as homogeneous might lead to a serious underestimation of the free energy of nuclei.^{2a} Apparently, the experimental nucleation rates for various colloidal approximants of the HS system scatter substantially (see, e.g., Figure 5 in Gong, T. Y.; Shen, J. G.; Hu, Z. B.; Marquez, M.; Cheng, Z. D. *Langmuir* **2007**, *23*, 2919), casting doubts to their relevance to the true HS system.

(44) Gránásy, L.; Pusztai, T.; James, P. F. *J. Chem. Phys.* **2002**, *117*, 6157.

(45) Laird, B. B. *J. Chem. Phys.* **2001**, *115*, 2887. Laird, B. B.; Davidchack, R. L. *J. Phys. Chem. B* **2005**, *109*, 17802.

JP8097439